

# Shock Attenuation Effectiveness by Simple Obstacles to Mitigate Severe Accident Explosive Loads

Jin-Su Kim\*, Jong-Woon Park

Dongguk univ., 707, Sekjang-Dong, Gyeong Ju, South Korea

\* Corresponding author: jinsur@gmail.com

## 1. Introduction

Fukushima accident showed that hydrogen explosions are no longer exclusive events in nuclear power plant severe accidents and additional creative safety features may be needed to preserve the integrity of vital components and structures against blast waves from the explosive events. Experimental and numerical studies for shock wave attenuations by simple geometrical means are previously performed [1, 2].

Based on these ideas, computational fluid dynamic analysis method is employed in the present work to investigate the plausibility of attenuations of shock waves that may occur in nuclear power plants by using simple obstacles. Following are the present method, results and important implications.

## 2. Benchmark Analyses of Shock Propagation

For the present shock wave analyses, FLUENT code [3] is utilized and thus benchmark analyses are firstly performed for the existing experimental conditions of the MSU shock tube [4], which simulates so called 'Riemann Problem'.

### 2.1 Riemann Problem

Representative fluid model for the MSU shock tube is shown in Fig. 1 consisting of high-pressure driving section, low-pressure driven section and the separating diaphragm in between. This model is a simplification of the originally three-section MSU shock tube [4].

Analyses of the physical behavior of a gas through the shock tube model in Fig. 1 are performed by using the full compressible Navier-Stokes equation of the FLUENT code with second-order accuracy in space [3]. Laminar and inviscid calculations are performed using the density based solver and the coupled explicit scheme [3]. For an ideal situation, the diaphragm bursting process, wall heat transfer and gas leakages are not considered. It is also assumed that air is an ideal gas and the tube walls and obstacles are rigid bodies.

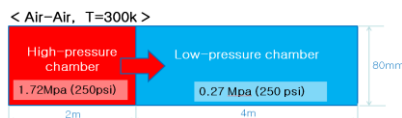


Fig. 1. Fluid domain for MSU shocktube [4].

Shock resolution capacity and mesh sensitivity are investigated using three mesh numbers, 2D and 3D and Adaptive Mesh Refinement (AMR) options. Analysis cases are summarized in Table 1. Basically, rectangular meshes are used. On the other hand, in the AMR, the meshes near high-gradient incident shock regions are

adaptively refined [3]. Computational time step size and viscous models are 60  $\mu$ s and laminar model for the 2D cases, and 30  $\mu$ s and inviscid model for the 3D case.

Table I: Computational options

	Viscosity	Mesh number	AMR	Time step size
2D	Laminar	7500	On	30 $\mu$ s
			Off	
		30000	Off	
3D	Inviscid	211,680	Off	60 $\mu$ s

Fig. 2 shows the pressure, density and temperature profiles along the tube length at an instant of the transient computed. They are nearly the same except for small differences at the discontinuities. The incident shock front and following contact surface typical of a general Riemann problem are well predicted with little dependence on computational options. It is thus decided that two-dimensional fixed 7500 meshes without AMR option is reasonably sufficient for engineering applications.

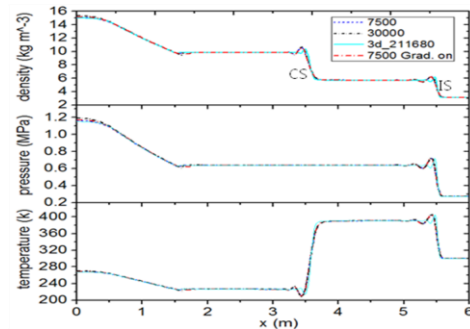


Fig. 2. Profiles of gas properties along the tube length (CS: contact surface; IS: Incident Shock)

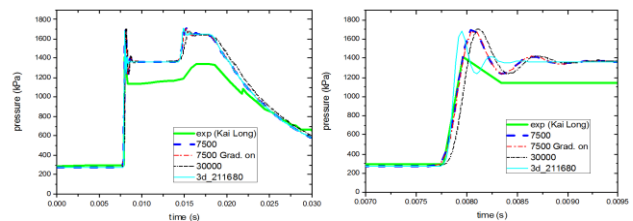


Fig. 3. Pressure variations at the right end of the tube

### 2.2 Comparison with Test Data

Pressure variations at the right end wall obtained from the experiment [4] and the present computations are shown in Fig. 3. All the computational cases show nearly identical results. Peak pressures from the computations range from 1.68 to 1.71 MPa whereas the peak pressure from the experiment is 1.41 MPa. This difference seems to be due to fluid losses from tube sealing and the non-prompt opening of the diaphragm in the experiment, which were not included in the present

ideal computations. Computational shock arrival times are 7.6-7.7 ms that are very close to the experiment of 7.8 msec. Heat loss effect is negligible.

### 3. Analyses of Shock Attenuation by Obstacles

#### 3.1 Multiple Obstacles

Effect of multiple obstacles on shock attenuation is analyzed. Several rectangular obstacles are positioned at a downstream of a small hypothetical 2D shock tube model. Fluid domain is shown in Fig 4. Rectangular meshes are used with 9,186 computational cells. Laminar viscous model is adopted. The computational result is compared with the case without obstacles.

Figure 5 shows snapshots of the pressure contours thus obtained. A part of incident shock is reflected backwards by the obstacles and the rest passing through the holes between the obstacles suffer from dispersions to radial directions. Fig. 6 shows the peak pressure variations at the right end wall for the two cases. The peak pressure without the obstacles is 1.937 MPa whereas the peak is reduced to 1.422 MPa for the case with the obstacles, which is 26.6% lower. Backward wave reflections would be a major reason of the peak pressure reduction. This result implies the plausibility of placing obstacles to attenuate the shock energy and applicability to reactor conditions. In the following section, this shock attenuation concept is extended to a reactor scale computations.

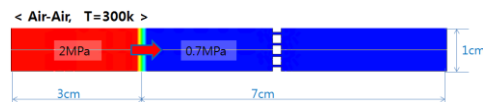


Fig. 4. Computational domain with multiple obstacles

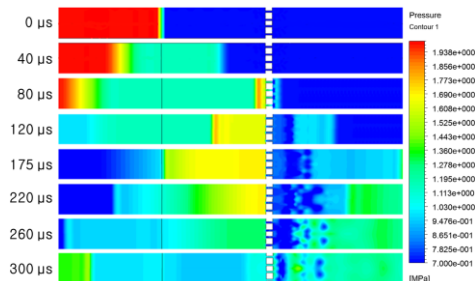


Fig. 5. Pressure contours for the case with multiple obstacles

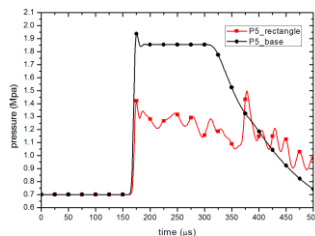


Fig. 6. Pressure variations at the right end wall for the cases with and without obstacles.

#### 3.2 Reactor Scale Analysis

A hypothetical two-dimensional reactor cavity is assumed for a reactor scale analysis. The cavity dimension is shown in the far left of Fig. 7. A high pressure source of 0.2 m radius semicircle is positioned at the central bottom the cavity to simulate a shock wave

generation. This mimics steam explosion triggered in water. However, in the present case the medium is assumed to be air mainly because the present analysis is only to observe the effect of presence of the obstacles.

Figure 7 shows the pressure contours snapshot at serial instances for the two cases with and without the obstacles. As in the previous section, incident circular shock wave is dispersed backwards and forwards from the obstacles. Figure 8 shows the pressure variations at the reactor bottom center (p1) and the 45° upper outer wall (p2). The peak pressures at p1 and p2 with the obstacles are 34.0% and 52.3% lower than the case without the obstacles, respectively.

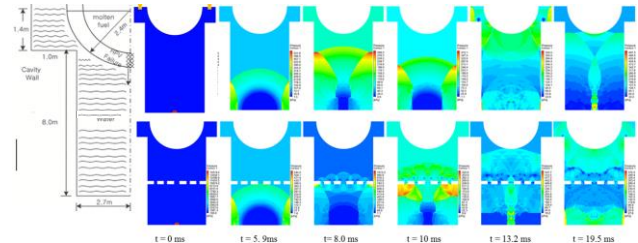


Fig. 7. Simplified reactor domain and pressure contour

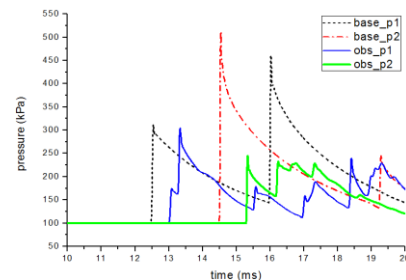


Fig. 8. Pressure variations at positions p1 and p2

### 4. Conclusions

Computational fluid dynamic analyses are employed to investigate the plausibility of shock attenuations by simple obstacles. Benchmarking and shock attenuation analyses for a simple geometry show reasonable accuracy and possibility of shock wave attenuation by obstacles. For a reactor scale application, it is found that the several rectangular obstacles can reduce peak pressures by 30~50% at the reactor bottom outer wall. This implies the feasibility of attenuating shock waves generated from the hydrogen and/or steam explosions in nuclear power plants under severe accidents. More elaborate computational analyses and experimental verification are desirable. These are planned for the future.

### REFERENCES

- [1] S. Berger, O. Sadot, G. Ben-Dor, Experimental investigation on the shock-wave load attenuation by geometrical means, *Shock Waves* 20, 29-40, 2010.
- [2] S. Sha, C. Zhihua, J. Xiaohai, H. Junli, Numerical investigations on blast wave attenuation by obstacles, *Procedia Engineering* 45, 453-457, 2012.
- [3] ANSYS FLUENT Theory Guide, ANSYS Inc., Canonsburg, 2011.
- [4] K. Long, Blast Simulation with Shock Tube Testing and Computational Fluid Dynamics Analysis, Master's Thesis, Michigan State University, 2008.